Design and breadboarding of a phased telescope array for free-space laser communications

Klaus H. Kudielka, Andras Kalmar, Walter R. Leeb
Institut für Nachrichtentechnik und Hochfrequenztechnik,
Technische Universität Wien
Gußhausstraße 25/389, A-1040 Wien

Abstract— **The design of a 16-aperture receive telescope array demonstrator for optical space communications is presented. Preliminary experimental results and computer simulations show that a telescope array with such dimensions and performance could be used as a receive terminal in a coherent optical interorbit link.**

Introduction

Space borne laser communication requires optical antennas in the form of telescopes. The envisaged telescope diameters are between $10cm$ and $30cm$, which implies antenna gains of some $120dB$ and beam widths on the order of a few microradian. Such extremely narrow characteristics ask for antenna pointing accuracies in the sub-microradian domain. Due to platform vibrations, transmitter/receiver tracking capabilities at frequencies up to several hundred Hertz have to be provided. As a result, pointing in free-space laser communication links turns out to be of equal or of even more importance than the task of data transmission and signal detection itself.

For the telescope realization so far mainly single ("monolithic") telescopes with mechanical fine-pointing mechanisms have been considered [1]. However, arranging several subtelescopes in close proximity and coherently superimposing the subsignals offer many fundamental advantages, such as smaller diameter of optical elements, reduced structural length, inherent modularity, and capability of inertia-free fine pointing.

Under contract of the European Space Agency (ESA) we are designing, manufacturing, and testing an engineering demonstrator of a phased telescope array to be used in the receive branch of a coherent intersatellite laser communication link. In the following we explain the basic concept of such a system, describe the design of our experimental setup, and give the most important performance parameters as predicted by computer simulation.

Basic Concept

Figure 1 shows the basic architecture of a phased receive telescope array with $N = 8$ subtelescopes. The subtelescopes collect the incident optical radiation and couple it into N piston actuators which allow to introduce phase shifts. Then the subbeams are superimposed by a beam combiner, i.e. a binary tree of $N - 1$ symmetric directional couplers. Both input ports of each coupler carry substantially equal powers. The signal output port nominally carries the total optical input power. The optical power in the control output port of each directional coupler is measured by a power sensor and actively minimized via a control loop.

The control unit shown in Figure 1 comprises $N - 1$ loop electronics. For each of the N piston actuator inputs, a linear combination of the resulting control signals is formed, effectively decoupling the piston control loops.

Simultaneous minimization of the optical powers within the $N - 1$ control output ports of the beam combiner gives the maximum optical power at the array output. The total optical power available from the subtelescopes is added coherently and directed to the subsequent receiver. As a result, the array's main lobe automatically follows the direction of the incident wavefront within a single subtelescope's field of view.

Besides piston adaption, the control unit of the phased receive telescope array fulfills the following tasks (see Figure 1):

- It checks and, if necessary, restores the relative coalignment of the subtelescope axes in regular intervals.
- It compensates for large, low-frequency pointing errors via a mechanical coarse-pointing mechanism. (The angular range covered by the phased telescope array itself is small compared to the a-priori pointing uncertainty).

Engineering Demonstrator Design

Table I shows the design goals given by the European Space Agency. Such a phased telescope array could be used, e.g., on a geostationary satellite receiving laser carried data from a low-earth-orbiting satellite at a rate of some $1Gbit/s$ [2].

The engineering demonstrator is designed to operate at a wavelength of $\lambda = 1.064\mu m$. Experiments will be performed only in the laboratory, although space-worthy concepts were applied wherever possible. The system consists of two principal units, i.e. the subtelescope array and the phasing unit.

Figure 2 shows the basic design of the subtelescope array. It consists of $N = 16$ aluminum tubes, each holding focussing optics and a motorized fiber launcher. The tubes are fixed on a baseplate at a 4×4 Cartesian grid, the optical axes are separated by $35mm$. The focussing optics, each comprising three lenses, have a clear aperture of $25mm$ and a focal length of $92.5mm$. At the operating wavelength, they

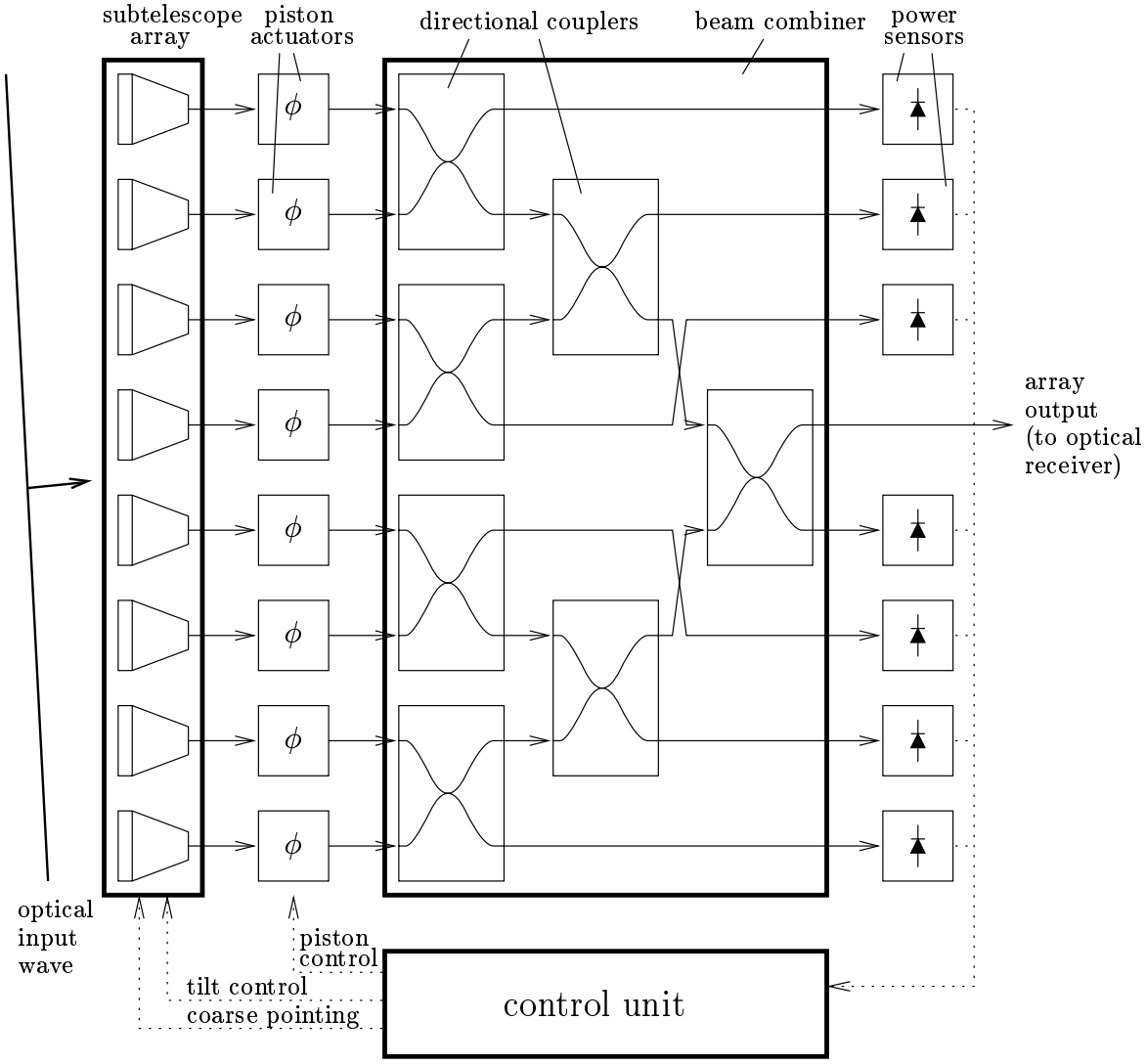

Fig. 1. Basic architecture of a phased receive telescope array

produce a spot with a diameter very close to the diffraction limit of $5.62\mu m$. After passing quarter-waveplates converting the circular input state of polarization into a linear one, the focussed optical radiation is coupled into polarization-maintaining single-mode fibers (PMF). The waveplates are glued directly to the fiber ends. Piezoelectrically driven screws (Model 8351, New Focus, USA) are used to individually shift each fiber end in both directions orthogonal to the optical axis, thus providing the possibility to automatically coalign all subtelescope axes.

The 16 fibers of the subtelescope array feed the phasing unit depicted in Figure 3 via polarization-maintaining single-mode fiber connectors.

Piston actuators will be realized by fiber stretchers, i.e. the PMF is wound around a piezo-electric tube which has silver elctrodes fired on. By applying a voltage, the diameter of the tube and thus the length of the fiber is changed. The fiber stretchers to be used have a diameter of $14mm$, a length of $10mm$, and a wall thickness of $1mm$. The first electro-mechanic resonance occurs at a frequency of $70kHz$. By optimizing the driver circuits we were able to achieve a step response with a settling time of $10\mu s$ and negligible overshoot.

The beam combiner will be made of five identical modules, each comprising three commercially available fiber directional couplers (Model 904P, Canadian Instrumentation and Research Ltd., Canada). The devices show very low insertion loss (about $0.1dB$ per coupler) and good symmetry. Fusion splices will interconnect piston actuators and combiner modules. Polarization-maintaining fiber connectors are mounted at the beam combiner's output fibers.

During nominal operation, i.e. when all optical phases are correctly set, no signal is diverted to the optical power sensors. Noise introduced by these modules results in piston errors and thus reduces the telescope array's output power. Using InGaAs photodiodes and low-noise operational amplifiers we designed and tested power sensors with a noise-equivalent input power of some $50fW/\sqrt{Hz}$ at a frequency of $20kHz$. This value guarantees efficient operation of the phased array even if the optical input power is

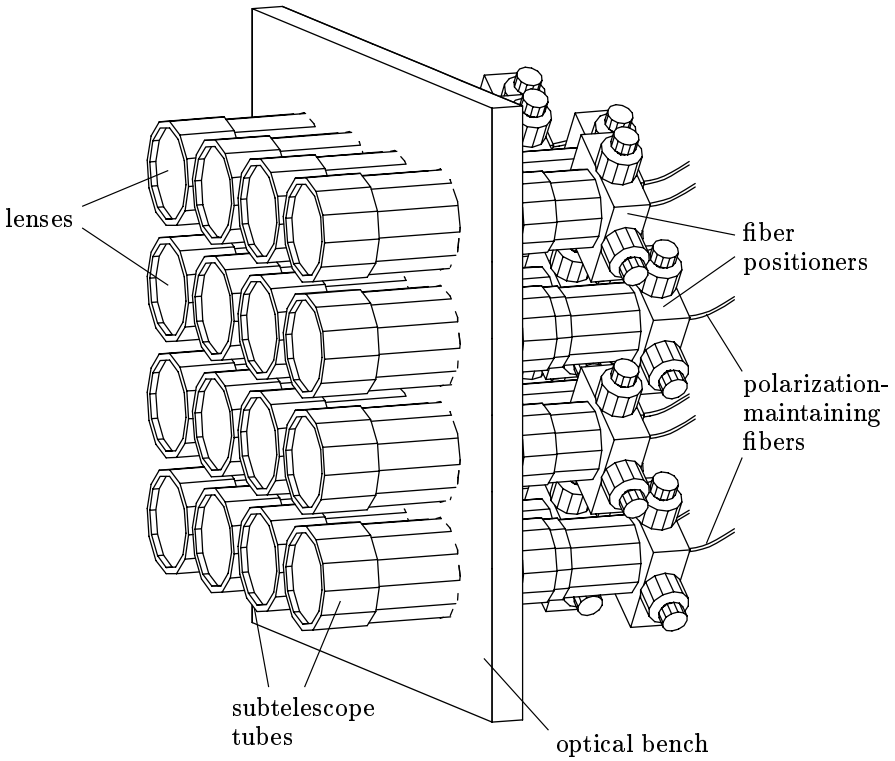

Fig. 2. Basic design of the subtelescope array

Parameter	Design goal
Wavelength	$0.8\mu m \ldots 1.1\mu m$
Equivalent aperture diameter	$10cm \ldots 16cm$
Number of subapertures	$8 \ldots 16$
Tracking angular range ($-1dB$ full angle)	$> 30\mu rad$
Spectral width of optical input	$1.3GHz$
State of polarization	circular
Optical input power on equivalent aperture	$10nW \ldots 200nW$
Optical throughput (input aperture to array output)	> 0.45
Tracking response ($-3dB$ closed-loop rejection cut-off frequency)	$> 2kHz$
Incoherent background noise ($\Delta\lambda = 5nm$)	$2 \cdot 10^{-2} pW/\mu rad^2$

TABLE I
DESIGN SPECIFICATIONS FOR THE ENGINEERING DEMONSTRATOR

as low as $10nW$ at the input aperture. The InGaAs photodiodes are equipped with multimode fibers and are coupled to the beam combiner outputs via fiber connectors.

The control unit drives the piston actuators such that the optical power detected by each of the 15 power sensors is minimized. A dither algorithm is used for minimum finding, i.e. a small periodic piston disturbance is applied to each of the 15 control loops [3]. The optical power variations occurring at each sensor are synchronously demodulated, resulting in a sinusoidal phase detector characteristic. Loop filters followed by integrators form 15 optical phase-locked loops. The 15 control signals are applied to the 16 piston actors via a linear network which serves to decouple the phase-locked loops. We have shown both by experiment [4] and by theoretical analysis [5] that it is sufficient to employ a single dither frequency for all control loops. For the engineering demonstrator we will use a dither frequency of $f_d = 20kHz$ and a dither amplitude of $\Delta\phi_d = 60mrad$. Hence the piston control algorithm, the optical power sensors, and the piston actuators will operate at a sample rate of $2 \cdot f_d = 40kHz$.

For simplicity, no coarse pointing mechanism will be implemented in the engineering demonstrator. However, the control unit provides an angle-of-incidence output which could be used in a coarse pointing control loop. By analyzing the piston control signals it estimates the optical input wave's angle of arrival. Due to thermal drifts between the individual subtelescope paths, the angle-of-incidence indicator has to be calibrated regularly, however.

A regular co-alignment of the subtelescope axes is performed by the control unit, too. To this end the phase-locked loops pertinent to the leftmost directional couplers are inverted (compare Figure 1). This causes the corresponding optical power sensors to be fed with the coherent sum of two subtelescope signals. The tilts of both subtelescopes are successively adjusted by laterally shifting the fiber ends within the subtelescopes for maximum optical power. Finally, the piston control loops are switched back

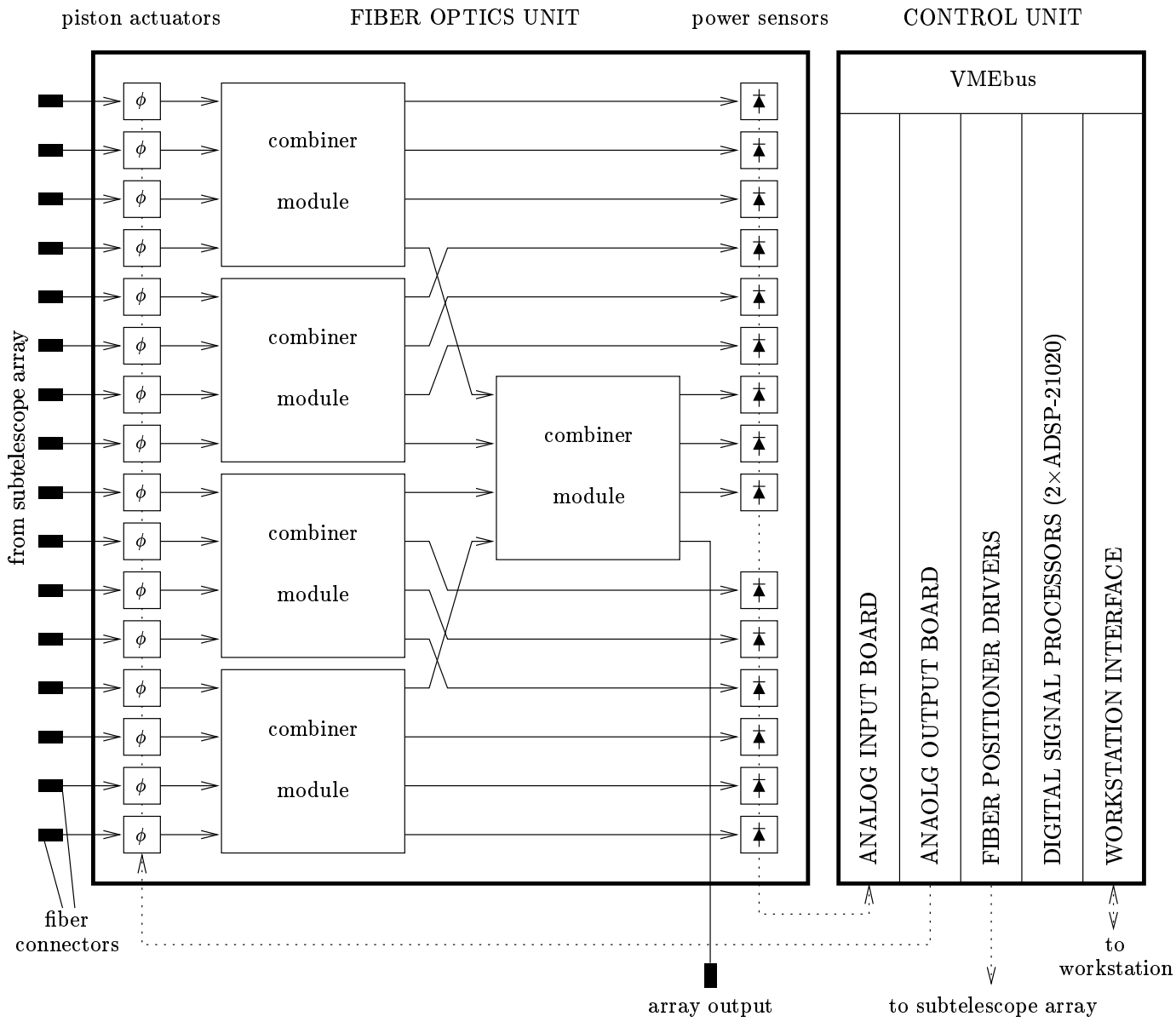

Fig. 3. Block diagram of the phasing unit

to normal polarity.

All the algorithms described above, i.e. piston control, angle of incidence indication, and subtelescope co-alignment will be implemented on a VMEbus-based system consisting of a dual-ADSP-21020 digital signal processor board (Model IXD7232, Ixthos, USA), custom analog input and output boards, and a subsystem driving the piezo-electric fiber positioners (see Figure 3).

Predicted Performance

With a number of preliminary experiments and computer simulations performed we expect the phased telescope array to achieve the high optical throughput required and to provide excellent phasing properties.

Using the design parameters given above, the subtelescope characteristic and the array characteristic expected for the engineering demonstrator are shown in Figure 4. During normal operation of the telescope array, the subtelescope path lengths are adapted automatically, and the angular dependence of the array output power is given by the subtelescope characteristic. The $-1dB$ tracking angular range thus amounts to $28\mu rad$, close to the ESA specification. For angular disturbances the control unit cannot adapt to, i.e. for variations above the phase-locked loops' cut-off frequency, the array characteristic applies.

Figure 5 depicts the predicted error response of the piston control loops. The response was determined by a time-domain simulation which also showed that the simultaneous operation of 15 control loops using a single dither frequency is feasible. The specified $-3dB$ cut-off frequency of $2kHz$ can be attained. This means that satellite vibrations, usually extending to a few hundred Hertz, will be sufficiently suppressed by the telescope array.

Since the optical power sensors introduce noise into the

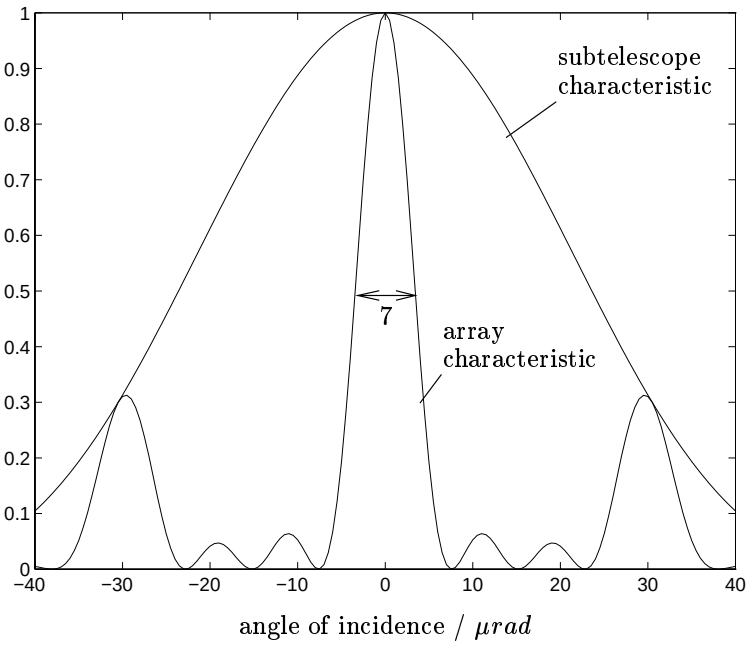

Fig. 4. Cross-section of the subtelescope characteristic and of the array characteristic

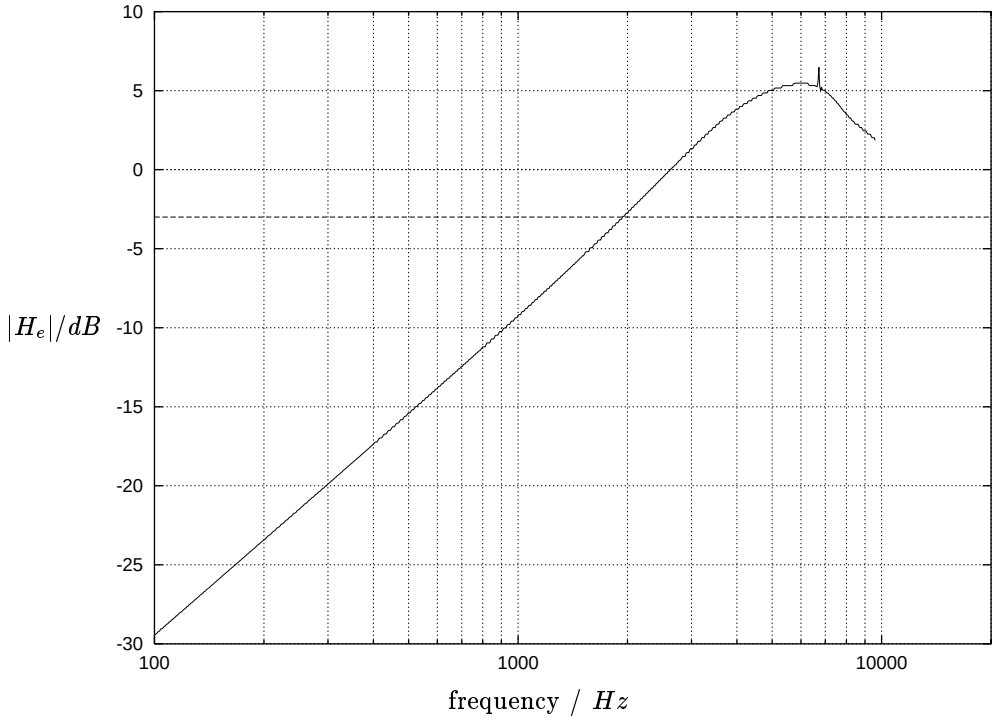

Fig. 5. Error response of the piston control loops of the engineering demonstrator. The sample rate amounts to $40kHz$.

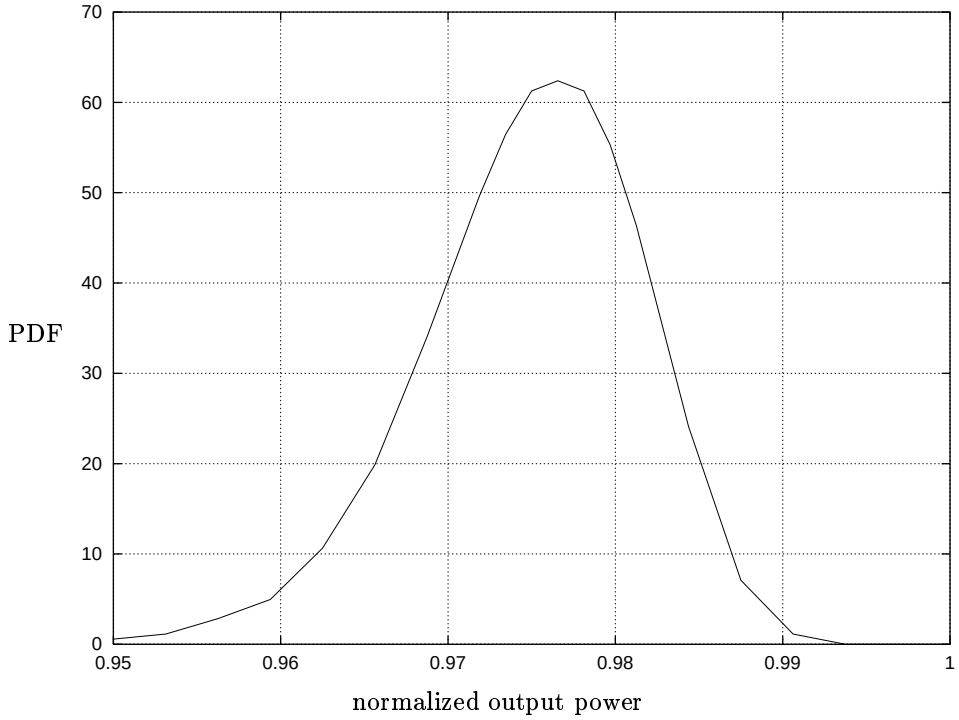

Fig. 6. Probability density function (PDF) of the normalized array output power

piston control loops and the subtelescope phases are slightly dithered, the array output power will be reduced. Using the time-domain simulation model, we calculated the probability density function (PDF) of the output power for the minimum optical input power of $10nW$. Figure 6 shows the result. The phasing efficiency, i.e. the ratio of the mean output power occurring in the real system to the output power in case all pistons are perfectly aligned, is expected to be greater than 97%. The probability that the output power is reduced by more than $0.3dB$ amounts to 10^{-6}.

Conclusion

Phased telescope arrays offer several advantages for coherent optical intersatellite communications, i.e. low mass, high modularity, and non-mechanical, adaptive pointing. We have presented the design of a 16-aperture receive telescope array demonstrator with characteristics aiming for application in space. Currently the subsystems are being manufactured.

Acknowledgement

The contents of this paper evolved from a research project supported by the European Space Agency. We wish to thank Bernhard Furch for monitoring and promoting this work.

References

[1] P. Gatenby et al., "Flight configuration for the small optical user terminal," in *Proc. SPIE*, 1994, vol. 2123, pp. 122–133.

[2] A. F. Popescu and B. Furch, "Status of the European developments for laser intersatellite communications," in *Proc. SPIE*, 1993, vol. 1866, pp. 10–20.

[3] T. R. O'Meara, "The multidither principle in adaptive optics," *J. Opt. Soc. Am.*, vol. 67, no. 3, pp. 306–315, March 1977.

[4] K. H. Kudielka et al., "Experimental verification of an adaptive optical multi-aperture receive antenna for laser space communications," in *Proc. SPIE*, 1994, vol. 2123, pp. 478–486.

[5] K. H. Kudielka et al., "Adaptive optical multi-aperture receive antenna for coherent intersatellite communications," in *Proc. SPIE*, 1994, vol. 2210, pp. 61–70.